Electronic structure and time-dependent description of rotational predissociation of LiH

P. Jasik, J. E. Sienkiewicz J. Domsta and N. E. Henriksen

The adiabatic potential energy curves of the $^1\Sigma^+$ and $^1\Pi$ states of the LiH molecule were calculated. They correlate asymptotically to atomic states, such as 2s + 1s, 2p + 1s, 3s + 1s, 3p + 1s, 3d + 1s, 4s + 1s, 4p + 1s and 4d + 1s. A very good agreement was found between our calculated spectroscopic parameters and the experimental ones. The dynamics of the rotational predissociation process of the $1^1\Pi$ state were studied by solving the time-dependent Schrödinger equation. The classical experiment of Velasco [*Can. J. Phys.*, 1957, **35**, 1204] on dissociation in the $1^1\Pi$ state is explained for the first time in detail.

1 Introduction

During the past twenty years, the physics of diluted gases have seen major advances in two fields, namely laser cooling of atomic and molecular samples and femtosecond chemistry. In both cases, appropriate frequency and phase-shaped laser light are used to control the system. In this context, two fundamental processes, *i.e.*, photoassociation and photodissociation, or in other words formation and breaking of the chemical bond by light, have attracted the attention of theoreticians, as well as experimentalists. In particular, photodissociation of diatomic or small polyatomic molecules is an ideal field for investigating molecular dynamics at a high level of precision.

Homonuclear and heteronuclear alkali metal molecules, including LiH, are valuable for theoreticians, mainly because they have a simple electronic structure, being two-valence electron systems. They can serve as convenient prototypes to test theoretical methods, which can be further applied to more complicated molecular systems. Besides that, knowledge of interatomic adiabatic potential energy curves of diatomic systems is essential for the understanding of several processes such as photodissociation, photoassociation, cooling and trapping. An extensive survey on the spectroscopy and structure of LiH was published in 1993 by Stwalley and Zemke,[1] and this was followed by a study by Gadea and Leininger[2] in 2006.

In 1935–1936, Crawford and Jorgensen[3,4] analysed the LiH band spectra. Since then, many notable studies have been undertaken. Among them, in 1962 Singh and Jain[5] applied the Rydberg–Klein–Rees method to obtain energies of the low excited states of LiH. Gadea and coworkers calculated potential energy curves,[2,6–8] radial couplings,[9] nonadiabatic energy shifts,[10] as well as LiH formation by radiative association in ion collisions.[11] Results of several other calculations, including semiempirical and *ab initio* approaches to describe important physical and chemical properties of LiH are available.[12–26] Calculations related to LiH are also used in the description of the formation of ultracold polar molecules in a single quantum state (*e.g.* Côté *et al.*[27]). Special investigations have been devoted to dipole moments[28,29] and the ionic states of LiH.[30–32] Tung *et al.*[33] and Holka *et al.*[34] performed very accurate calculations of the ground and some excited state potential curves.

LiH was also intensively explored in time-dependent studies. Again, being only a four-electron molecule makes it a convenient example for molecular dynamics calculations. In 1936, Mulliken[35] noted that the change in the internuclear separation may cause a rearrangement in the distribution of the density of electrons. Recently, the LiH molecule was used in a computational study using the time-dependent multiconfiguration method.[36]

The aim of our work was to provide accurate potential energy curves and to use them to explain a classical experiment by Velasco[37] on rotational predissociation. We chose to solve the time-dependent Schrödinger equation (TDSE) with a probe wavepacket placed on the effective interatomic potential possessing a centrifugal barrier. This approach made it possible to compare rovibrational spacings with the results derived from the experiment by Velasco[37] and with those calculated directly from the electronic structure. Our work was also motivated by the case of the NaI molecule intensively studied by A. Zewail[38] and later by others.[39–42] The NaI dimer shows similar behavior to LiH in creating ionic bonds and is a well-studied prototype molecule in femtochemistry, particularly in relation to the dynamics of unimolecular reactions.

In Section II, the appropriate model of the electronic structure is defined, leading to an algorithm for the calculation of some low-excited singlet Σ^+ and Π states. Later, we describe the theoretical backgrounds of rotational predissociation and molecular dynamics. We explain how the obtained adiabatic potentials can be used in the theoretical treatment of the rotational predissociation proccess. In particular, we present a method for the calculation of the dynamics of predissociation of molecules starting with a given coherent wavepacket. In Section III, we present the rotational predissociation results for the $1^1\Pi$ state and compare them with the measurements of Velasco.[37] Conclusions are given in the last section.

2 The model

2.1 Electronic structure

We consider the interaction between the lithium (atom A) and hydrogen (atom B) under the assumption that the molecular state is a composition of the electronic adiabatic states $\Psi_i^{\mathrm{el}}(\vec{r};R)$, $i = 1, 2, 3, \ldots$, which depend on the positive variable R, *i.e.* on the separation between the nuclei of these atoms. The applied notation indicates that our considerations are restricted to such eigenstates, which are independent of the direction of the vector joining the nuclei. In other words, electronic wave functions possess spherical symmetry with respect to the nuclear coordinates. Our calculations are based on the Born–Oppenheimer approximation, *i.e.* the solutions of the following time-independent Schrödinger equation:

$$H^{\mathrm{el}}\Psi_i^{\mathrm{el}}(\vec{r};R) = E_i^{\mathrm{el}}(R)\Psi_i^{\mathrm{el}}(\vec{r};R). \tag{1}$$

Here, the separation parameter R is kept fixed, vector $\vec{r}$ represents all the electronic coordinates, H^{el} is the electronic Hamiltonian of a diatomic system. Thus, $\Psi_i^{\mathrm{el}}(\vec{r};R)$ describes the ith eigenstate of the Hamiltonian, $E_i^{\mathrm{el}}(R)$ are the corresponding eigenvalues, also called adiabatic potentials. The Hamiltonian of the system can be written as

$$H^{\mathrm{el}} = T^{\mathrm{el}} + V, \tag{2}$$

where T^{el} stands for the kinetic energy operator of the valence electrons and V represents the operator of the interaction between the valence electrons, the Li-core and the nucleus of H. In the present approach only the valence electrons are treated explicitly, which allows for an adequate description of electron correlation at low computational cost. The lithium core is represented by an angular momentum-dependent pseudopotential. The latter is obtained as

$$V = V^{\mathrm{A}} + V_{\mathrm{pol}}^{\mathrm{A}} + V^{\mathrm{B}} + \frac{1}{r_{12}} + V_{\mathrm{cc}}. \tag{3}$$

Here, V^{A} describes the Coulomb and exchange interaction as well as the Pauli repulsion between the valence electrons and the lithium core. We use the following semi-local energy-consistent pseudopotentials:

$$V^{\mathrm{A}} = \sum_{i=1}^{2} \left(-\frac{Q_{\mathrm{A}}}{r_{\mathrm{A}i}} + \sum_{l,k} B_{l,k}^{\mathrm{A}} \exp\left(-\beta_{l,k}^{\mathrm{A}} {r_{\mathrm{A}i}}^2\right) P_l^{\mathrm{A}} \right), \tag{4}$$

where $Q_{\mathrm{A}} = 1$ denotes the net charge of the lithium core, P_l^{A} is the projection operator onto the Hilbert subspace of angular symmetry l with respect to the Li^+-core. The parameters $B_{l,k}^{\mathrm{A}}$ and $\beta_{l,k}^{\mathrm{A}}$ define the semi-local energy-consistent pseudopotential. The second interaction term in eqn (3) is the polarization term that describes, among others, core-valence correlation effects and is calculated as

$$V_{\mathrm{pol}}^{\mathrm{A}} = -\frac{1}{2}\alpha_{\mathrm{A}}\vec{F}_{\mathrm{A}}{}^2, \tag{5}$$

where $\alpha_{\mathrm{A}} = 0.1915a_0$ is the dipole polarizability of the lithium core[43] and $\vec{F}_{\mathrm{A}}$ is the electric field generated at its site by the valence electrons. For the latter we use the following formula:

$$\vec{F}_{\mathrm{A}} = \sum_i \frac{\vec{r}_{\mathrm{A}i}}{{r_{\mathrm{A}i}}^3}\left[1 - \exp\left(-\delta_{\mathrm{A}}{r_{\mathrm{A}i}}^2\right)\right], \tag{6}$$

where δ_{A} is the cutoff parameter, which equals $0.831{a_0}^{-2}$ (value taken from Fuentealba *et al.*[43]). The third term in eqn (3) represents the Coulomb interaction between the valence electrons and the hydrogen nucleus. The fourth term stands for the repulsion between the valence electrons, whereas the last term describes the interaction between the lithium core and hydrogen nucleus. Since the lithium atomic core and the hydrogen nucleus are well separated, we choose a simple point-charge Coulomb interaction in the latter case. More detailed characteristics of the applied potentials are given in the papers by Czuchaj and coworkers[44,45] and Dolg.[46]

The core electrons of the Li atom are represented by the pseudopotential ECP2SDF,[43] which was formed from the uncontracted (9s9p8d3f) basis set. The basis for the s and p orbitals, which comes with this pseudopotential, is enlarged by the functions for d and f orbitals given by D. Feller[47] and assigned by cc-pV5Z. Additionally, our basis set was augmented by four s short-range correlation functions (1979.970927, 392.169555, 77.676373, 15.385230), four p functions (470.456384, 96.625417, 19.845562, 4.076012), four d functions (7.115763, 3.751948, 1.978298, 1.043103) and four f functions (2.242072, 1.409302, 0.885847, 0.556818). Also, we added to the basis the following set of diffuse functions: two s functions (0.010159, 0.003894), two p functions (0.007058, 0.002598), two d functions (0.026579, 0.011581) and two f functions (0.055000, 0.027500). The numbers in parenthesis are the coefficients of the exponents of the primitive Gaussian orbitals. The basis set for the hydrogen electron is the standard cc-pV5Z basis.[48]

The spin–orbit coupling (SO) contributes insignificantly to the energy of our system, so we do not take it into account. To calculate the adiabatic potential energy curves of the LiH diatomic molecule, we use the multiconfigurational self-consistent field/complete active space self-consistent field (MCSCF/CASSCF) method and the multi-reference configuration interaction (MRCI) method. All the calculations are performed by means of the MOLPRO program package.[49] Using these computational methods we obtained adiabatic potential energy curves for singlet Σ^+ and Π states, which correlate to the Li(2s) + H(1s) ground atomic asymptote and the Li(2p) + H(1s), Li(3s) + H(1s), Li(3p) + H(1s), Li(3d) + H(1s), Li(4s) + H(1s), Li(4p) + H(1s) and

Table 1 Comparison of asymptotic energies with other theoretical and experimental results. Energies are shown in cm^{-1} units

Atomic asymptotes	Experiment Moore[50]	Theory Boutalib[6]	Theory Gadea[2]	Theory present
Li(2p) + H(1s)	14 904	14 905	14 898	14 904
Li(3s) + H(1s)	27 206	27 210	27 202	27 202
Li(3p) + H(1s)	30 925	30 926	30 920	30 921
Li(3d) + H(1s)	31 283	31 289	31 279	31 276
Li(4s) + H(1s)	35 012	35 018	35 007	35 016
Li(4p) + H(1s)	36 470	36 475	36 465	36 464
Li(4d) + H(1s)	36 623	37 590	36 626	36 617

Li(4d) + H(1s) excited atomic asymptotes, respectively. The quality of our calculations can be confirmed by the comparison with experimental and theoretical asymptotic energies for different electronic states, which is shown in Table 1. Our asymptotic energies for ground and excited states are in very good agreement with experimental and other theoretical values. In particular, a perfect match is found between our result and the experimental value for the Li(2p) energy level.

2.2 Rotational predissociation

When the adiabatic potential $E^{el}(R)$ of the singlet state $^1\Lambda$ is obtained from the solution of eqn (1), the effective potential energy may be written in the following form (*e.g.* Landau and Lifshitz):[51]

$$U_J(R) = E^{el}(R) + \frac{J(J+1) - \Lambda^2}{2\mu R^2}, \tag{7}$$

where Λ is the component of the sum over all the electron angular momenta on the diatomic axis, $J \geq \Lambda$ is the rotational quantum number of the molecule and μ is the reduced mass of the nuclei.

Rovibrational energies $E(v,J)$ depend on $E^{el}(R)$ as well as on vibrational v and rotational J quantum numbers. They are the solutions of the time-independent nuclear Schrödinger equation

$$H_J^{nuc}\Psi_{v,J}^{nuc}(R) = E(v,J)\Psi_{v,J}^{nuc}(R), \tag{8}$$

where the nuclear Hamiltonian is obtained as

$$H_J^{nuc} = -\frac{\hbar^2}{2\mu}\frac{\partial^2}{\partial R^2} + U_J(R). \tag{9}$$

The effective potential $U_J(R)$ forms a barrier for $J > 0$ with a maximum $U_J(R_J)$, at the internuclear distance R_J, which can easily be estimated. Any rovibrational state with a positive energy $E(v,J)$ lower than $U_J(R_J)$ has a finite lifetime before it will be decomposed due to a quantum tunneling effect. These states are called quasibound states and formally belong to the continuum. What is important is that during their lifetimes they can be regarded as bound states. When the energy $E(v,J)$ exceeds the barrier maximum $U_J(R_J)$, any bound state is not possible. Following Way and Stwalley,[52] we introduce a critical value of the rotational quantum number J_c, which obeys the two following inequalities:

$$E(v,J_c) < U_{J_c}(R_{J_c}) \tag{10}$$

and

$$E(v,J_c + 1) > U_{J_c+1}(R_{J_c+1}). \tag{11}$$

In other words, for a given v, the state with the energy $E(v,J_c)$ is the last of the quasibound states series supported by the barrier, and the state with the energy $E(v,J_c + 1)$ already belongs to the continuum. By solving eqn (8) we obtain $E(v,J_c)$ and estimate $E(v,J_c + 1)$. The differences $E(v,J_c) - E(0,0)$ and $E(v,J_c + 1) - E(0,0)$ may refer to the last observed and the first unobserved rotational predissociation experimental results, respectively.

2.3 Molecular dynamics

The time-dependent approach that is mathematically equivalent to the time-independent one can be regarded as a complementary tool and is often used in studying photodissociation processes. Here, it serves as an alternative and quite illustrative method for testing the results of our structural calculations.

We start our consideration from the time-dependent Schrödinger equation written in the following form:

$$\imath\hbar\frac{\partial}{\partial t}\Phi(R,t) = H_J^{nuc}\Phi(R,t), \tag{12}$$

for each $J \leq J_c$ separately, where $\Phi(R,t)$ is the time-dependent wavepacket moving on the effective potential energy curve $U_J(R)$ (eqn (7)) and H_J^{nuc} is the nuclear Hamiltonian given in eqn (9).

By definition, the wavepacket is a coherent superposition of stationary states (*e.g.* Tannor[53]), which may be represented in the following form consisting of two contributions from the discrete and continuous parts of the spectrum:

$$\Phi(R;t) = \sum_{v,J} c_{v,J}\Psi_{v,J}^{nuc}(R)e^{-\imath E(v,J)t/\hbar} + \int c_J(E)\Psi_{E,J}(R)e^{-\imath Et/\hbar}dE, \tag{13}$$

where

$$c_{v,J} = \int_0^\infty \Psi_{v,J}^{nuc}(R)^*\Phi(R;0)dR$$

and

$$c_J(E) = \int_0^\infty \Psi_{E,J}(R)^*\Phi(R;0)dR$$

are the energy-dependent coefficients, squares of these coefficients form the spectral distribution of Φ normalized to 1, $e^{-\imath E(v,J)t/\hbar}$ and $e^{-\imath Et/\hbar}$ are the time evolution factors, and $\Psi_{v,J}^{nuc}(R)$ and $\Psi_{E,J}(R)$ are eigenfunctions of $H_J^{nuc}(R)$. The wavepacket $\Phi(R;t)$ is a solution of eqn (12) and its initial shape at $t = 0$ is taken as a Gaussian function of arbitrary half-width placed on the effective potential energy curve. The wavepacket moves away from its starting location due to the Newtonian force $-dU_J/dR$. This process is described by the time-dependent autocorrelation function

$$S(t) = \int \Phi(R;t=0)\Phi(R;t)dR. \tag{14}$$

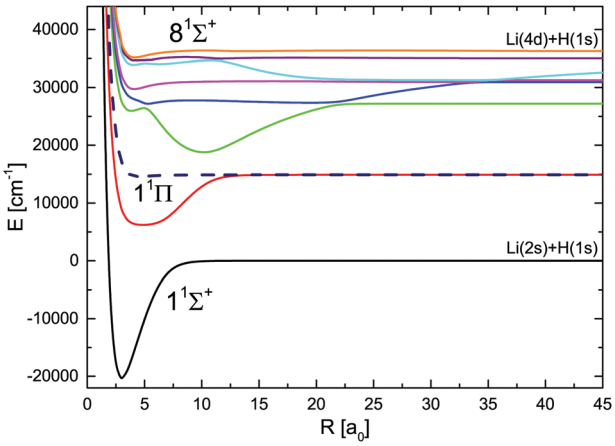

Fig. 1 Adiabatic potential energy curves of LiH: 1–$8^1\Sigma^+$ states (solid lines), $1^1\Pi$ state (dashed line).

In our case, the autocorrelation function describes evolution of the initial nuclear wavepacket in the excited electronic state. The time-dependent population in the range till R_{max} for the particular state labeled by J, in accordance with the effective potential energy U_J from eqn (7), is calculated as

$$P(t) = \int_0^{R_{max}} |\Phi(R;t)|^2 \mathrm{d}R. \quad (15)$$

We determine the discrete spectrum by the inverse Fourier transform of $S(t)$[54] as follows:

$$\sigma(E(\nu,J)) = |c_{\nu,J}|^2 = \lim_{T\to\infty} \frac{1}{T}\int_{-T/2}^{+T/2} \mathrm{e}^{\mathrm{i}E(\nu,J)t/\hbar} S(t)\mathrm{d}t \quad (16)$$

In our calculations of the autocorrelation function (eqn (14)), the propagation time is 150 ps, which is sufficient for the estimation of the integral in eqn (16). In eqn (15), we set the value of R_{max} to be equal to $100a_0$. There are 2^{12} points in the integration grid. To avoid the diffraction between the outgoing waves and the incoming ones due to bouncing from the boundary at R_{max}, a negative imaginary potential is placed at $90a_0$. This potential smoothly absorbs the wavepacket near the boundary.[55]

Table 2 Spectroscopic parameters R_e [a_0], D_e, ω_e, and T_e [cm^{-1}] for the ground and low-excited states of the LiH molecule

State	Dissociation limit	Author	R_e	D_e	ω_e	T_e
$1^1\Sigma^+$	Li(2s) + H(1s)	Present (theory)	3.003	20 327	1391	
		Dulick 1998 (exp.)[56]	3.014	20 286	1405	
		Stwalley 1993 (exp.)[1]	3.015	20 288	1407	
		Grofe 2017 (theory)[26]	3.024[a]	17 930[a]		
			3.001[b]	19 753[b]		
		Bande 2010 (theory)[25]	3.013	20 333		
		Aymar 2009 (theory)[23]	3.002	20 167	1398	
		Gadea 2006 (theory)[2]	3.003	20 349		
		Dolg 1996 (theory)[14]	3.000	20 123	1391	
		Boutalib 1992 (theory)[6]	3.007	20 174		
$2^1\Sigma^+$	Li(2p) + H(1s)	Present (theory)	4.866	8687	260	26 544
		Stwalley 1993 (exp.)[1]	4.906	8679		
		Grofe 2017 (theory)[26]	4.724[a]	7662[a]		23 551[a]
			4.250[b]	8469[b]		26 132[b]
		Bande 2010 (theory)[25]	5.173	8679		26 584
		Aymar 2009 (theory)[23]	4.820	8698	241	
		Gadea 2006 (theory)[2]	4.862	8687		
		Boutalib 1992 (theory)[6]	4.847	8690		26 390
		Vidal 1982 (theory)[13]	4.910	8686	244	
$1^1\Pi$		Present (theory)	4.50	286	226	34 945
		Velasco 1957 (exp.)[37]	4.49	284	216	
		Aymar 2009 (theory)[23]	4.52	251	243	
		Vidal 1982 (theory)[13]	4.50	289		
$3^1\Sigma^+$	Li(3s) + H(1s)	Present (theory)	3.821	1270	540	46 259
			10.172	8438	293	39 092
		Huang 2000 (exp.)[57]	—	—		
			10.140	8469		
		Grofe 2017 (theory)[26]	4.016[a]	−1371[a]		47 425[a]
			4.001[b]	1129[b]		45 570[b]
			9.449[a]	7662[a]		38 553[a]
			9.997[b]	8711[b]		42 021[b]
		Aymar 2009 (theory)[23]	3.830	1267	390	
			10.150	8361	390	
		Gadea 2006 (theory)[2]	3.821	—		
			10.181	8453		
		Boutalib 1992 (theory)[6]	3.825	1277		46 109
			10.206	8444		38 942

[a] MSDFT. [b] MS-CASPT2.

A normalized Gaussian-shaped wavepacket Φ is initially centered at $6.15a_0$ and possesses the half-width equal to $0.95a_0$.

3 Results and discussion

Our results of the calculated adiabatic potential energy curves of 1–$8\,^1\Sigma^+$ and $1\,^1\Pi$ states are presented in Fig. 1. Several characteristic avoided crossings are visible, particularly the double one at 5 and $20a_0$ between the curves of the $3\,^1\Sigma^+$ and $4\,^1\Sigma^+$ states. Although not very pronounced, there are avoided crossings between $1\,^1\Sigma^+$ and $2\,^1\Sigma^+$ at $7.5a_0$ and $2\,^1\Sigma^+$ and $3\,^1\Sigma^+$ at $10a_0$. Additionally, in Fig. 1, the ionic character of the molecular bond is clearly visible for larger R.

To benchmark our electronic structure calculations, bond lengths R_e, dissociation energies D_e, vibrational constants ω_e and electronic term energies T_e are compared with other theoretical and experimental results in Table 2. For the ground state our position of R_e agrees exactly with the theoretical value of Gadea and Leininger[2] and reasonably with the experimental values of Stwalley *et al.*[1] and Dulick *et al.*[56] We also find good agreement within 40 cm^{-1} between the well depths D_e of our results and the experimental data of Stwalley *et al.* In the case of $1\,^1\Pi$, our results of R_e and D_e agree within $0.01a_0$ and 2 cm^{-1} with the experimental data of Velasco, respectively. All the theoretical results indicate the existence of a double well for the $3\,^1\Sigma^+$ state, but this is not confirmed by the only available experiment by Huang *et al.*[57] A key observation is that for the state of interest, namely $1\,^1\Pi$, the excellent consistency between our results and the experimental data is better than for any previous theoretical results.

Fig. 2 displays spacings between successive rovibrational levels of the $1\,^1\Pi$ state. Our first set of values was obtained by solving[58] eqn (8). The second set comes from the appropriate differences between the positions of peaks in the absorption spectrum obtained from eqn (16) and presented in Fig. 3. These two sets agree very well

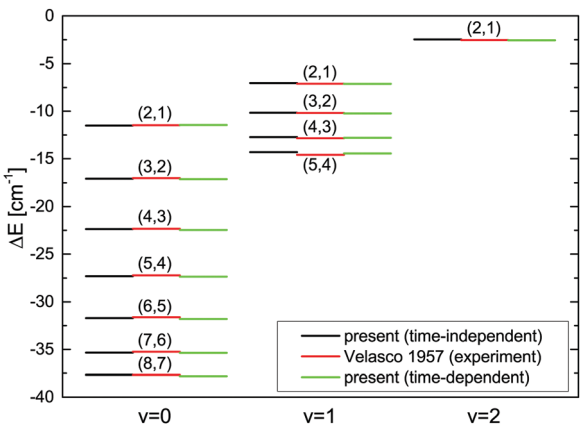

Fig. 2 Differences $\Delta E(v,J',J) = E(v,J') - E(v,J)$ between rovibrational levels with the same vibrational quantum number v of the $1\,^1\Pi$ state. Three series of differences are drawn for $v = 0$, 1 and 2. Each difference is specified by (J,J'). The black lines were derived from the calculated rovibrational levels. The red lines were derived from the experimental data of Velasco.[37] The green lines represent our results obtained from the absorption spectrum shown in Fig. 3.

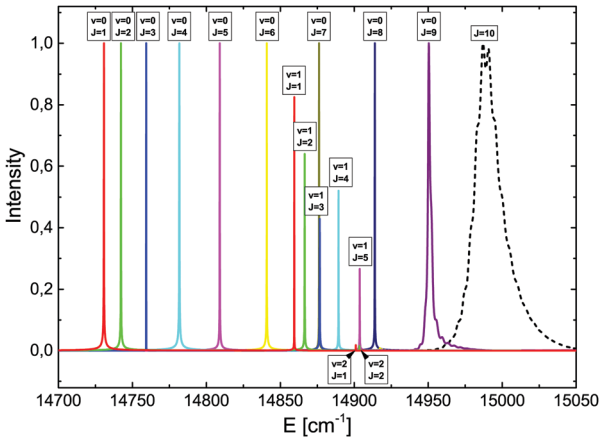

Fig. 3 The discrete spectrum calculated from eqn (16).

with each other. Moreover, there is also very good agreement with the experimental values of Velasco.[37]

The peaks in the spectrum (Fig. 3) were obtained by solving the time-dependent Schrödinger equation[55] (eqn (12)) in combination with eqn (16). Here, we are not interested in the intensity of the peaks and the precise shape of the initial wavepacket is unimportant. The set of effective potentials U_J (eqn (7)) spans J from 1 to 10. The broadened peak labeled by $v = 0$ and $J = 9$ is the last in the series since $J = 9$ is a critical value J_c, discussed in Section 2.2. Its half-width (FWHM) is equal to 2.7 cm^{-1}. The last very broad peak with $J = 10$ illustrates the situation where the depth of the effective potential is too shallow to allow for existence of any bound vibrational level. The last and already broadened peak observed by Velasco was assigned as $v = 0$ and $J = 8$. In his analysis, he correctly foresaw the existence of an unobserved peak labeled by $v = 0$ and $J = 9$ before the molecule breaks off due to high rotations. However, his prediction of the existence of two other missing peaks in the spectrum, namely with $v = 1$, $J = 6$ and $v = 2$, $J = 3$, is not confirmed by our results. The broadening of the peak with $v = 0$ and $J = 9$ shown by our calculation is due to quantum tunneling through the centrifugal barrier.

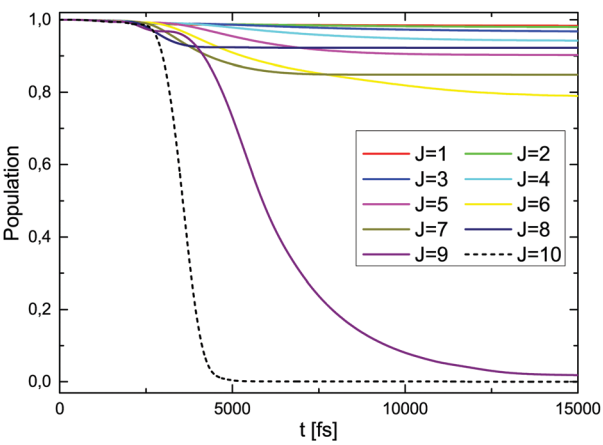

Fig. 4 Time-dependent population of the wavepacket placed on the effective potential $U_J(R)$ ($J = 1,\ldots,10$) for the electronic energy of the $1\,^1\Pi$ state. All the lines refer to the same initial conditions at $t = 0$ of the wavepacket.

The last figure (Fig. 4) shows the results for the time-dependent population of the $1^1\Pi$ state for the same initial condition. For $J = 10$, no bound states are supported by the effective potential and the drop in population around 2.5 ps shows the time it takes for the continuum wavepacket to reach $R = R_{max}$.

In all the cases, the population is close to the one within the first approximately 2.5 ps, since any continuum part of the wavepacket needs this time to reach R_{max}. Furthermore for low values of J, the population is close to the one within the time window of 15 ps, meaning that essentially all parts of the wavepacket can be represented by bound states. For $J = 9$, the wavepacket consists of a continuum as well as a (quasi-) bound part. The quasibound part decays through tunneling, giving rise to the slow exponential decay with a decay constant of 2.4 ps. On the basis of the time-energy uncertainty principle, we can estimate that this lifetime should give rise to a line width of approximately 2 cm^{-1}. This is in good agreement with the spectrum in Fig. 3.

4 Conclusions

To describe the rotational predissociation process of the LiH molecule, we started by calculating the low-lying adiabatic potential energy curves, with particular emphasis on the $1^1\Pi$ state. Our spectroscopic parameters are in very good agreement with the experimental values. Having the potential curve of $1^1\Pi$ state, we calculated the rovibrational levels. The differences between these successive levels were compared with those derived from the experimental data of Velasco. The agreement again was very good, which means that the shape of the first excited electronic state $1^1\Pi$ is reliable. On the other hand, since our difference (T_e) between the potential wells of $1^1\Pi$ and of the ground state $1^1\Sigma^+$ is around 50 cm^{-1} larger than the experimental value of Stwalley *et al.*, the direct comparison with the spectrum of Velasco shows a small systematic shift.

To gain insight into the complementary time-dependent approach, we solved the time-dependent nuclear Schrödinger equation. The solution shows the evolving wavepacket originally placed on the effective potential curve. The spectrum was calculated as a Fourier transform of the autocorrelation function. The differences between the successive peaks in the spectrum were compared with those of Velasco and ours obtained in the time-independent approach. All three sets of values are in very good agreement. Our results for the time-dependent population of the $1^1\Pi$ state explain in detail the rotational predissociation mechanism of the LiH molecule. A challenge for experimentalists would be to detect in real time (*via* pump–probe spectroscopy) the predissociation due to quantum tunneling through the centrifugal barrier.

Acknowledgements

This work was partially supported by the COST action XLIC (CM1204) of the European Community. The calculations were carried out using the resources of the Academic Computer Centre in Gdańsk.

References

1 W. C. Stwalley and W. T. Zemke, *J. Phys. Chem. Ref. Data*, 1993, **22**, 87.
2 F. X. Gadea and T. Leininger, *Theor. Chem. Acc.*, 2006, **116**, 566.
3 F. H. Crawford and T. Jorgensen Jr, *Phys. Rev.*, 1935, **47**, 932.
4 F. H. Crawford and T. Jorgensen Jr, *Phys. Rev.*, 1936, **49**, 745.
5 N. L. Singh and D. C. Jain, *Proc. Phys. Soc., London*, 1962, **79**, 753.
6 A. Boutalib and F. X. Gadea, *J. Chem. Phys.*, 1992, **97**, 1144.
7 M. E. Casida, F. Gutierrez, J. Guan, F. X. Gadea, D. Salahub and J. P. Daudey, *J. Chem. Phys.*, 2000, **113**, 7062.
8 H. Beriche and F. X. Gadea, *Eur. Phys. J. D*, 2016, **70**, 2.
9 F. X. Gadea and A. Boutalib, *J. Phys. B: At., Mol. Opt. Phys.*, 1993, **26**, 61.
10 F. Gemperle and F. X. Gadea, *Europhys. Lett.*, 1999, **48**, 513.
11 A. S. Dickinson and F. X. Gadea, *Mon. Not. R. Astron. Soc.*, 2000, **318**, 1227.
12 B. O. Roos and A. J. Sadlej, *J. Chem. Phys.*, 1982, **76**, 5444.
13 C. R. Vidal and W. C. Stwalley, *J. Chem. Phys.*, 1982, **77**, 883.
14 M. Dolg, *Theor. Chem. Acc.*, 1996, **93**, 141.
15 F. A. Gianturco and P. Gori Giorgi, *Phys. Rev. A: At., Mol., Opt. Phys.*, 1996, **54**, 4073.
16 F. A. Gianturco, P. Gori Giorgi, H. Berriche and F. X. Gadea, *Astron. Astrophys., Suppl. Ser.*, 1996, **117**, 377.
17 P. C. Stancil and A. Dalgarno, *Astrophys. J.*, 1997, **479**, 543.
18 A. K. Sharma and S. Chandra, *J. Phys. B: At., Mol. Opt. Phys.*, 2000, **33**, 2623.
19 E. Bodo, F. A. Gianturco and R. Martinazzo, *Phys. Rep.*, 2003, **384**, 85.
20 S. Bubin and L. Adamowicz, *J. Chem. Phys.*, 2004, **121**, 6249.
21 R. Fondermann, M. Hanrath and M. Dolg, *Theor. Chem. Acc.*, 2007, **118**, 777.
22 J. R. Trail and R. J. Needs, *J. Chem. Phys.*, 2008, **128**, 204103.
23 M. Aymar, J. Deiglmayr and O. Dulieu, *Can. J. Phys.*, 2009, **87**, 543.
24 I. L. Cooper and A. S. Dickinson, *J. Chem. Phys.*, 2009, **131**, 204303.
25 A. Bande, H. Nakashima and H. Nakatsuji, *Chem. Phys. Lett.*, 2010, **496**, 347.
26 A. Grofe, Z. Qu, D. G. Truhlar, H. Li and J. Gao, *J. Chem. Theory Comput.*, 2017, **13**, 1176.
27 R. Côté, E. Juarros and K. Kirby, *Phys. Rev. A: At., Mol., Opt. Phys.*, 2010, **81**, 060704.
28 M. Cafiero and L. Adamowicz, *Phys. Rev. Lett.*, 2002, **88**, 033002.
29 F. M. Fernandez, *J. Chem. Phys.*, 2009, **130**, 166101.
30 P. Decleva and A. Lisini, *J. Phys. B: At. Mol. Phys.*, 1986, **19**, 981.
31 S. Magnier, *J. Phys. Chem.*, 2004, **108**, 1052.
32 M. Cheng, J. M. Brown, P. Rosmus, R. Linguerri, N. Komiha and E. G. Myers, *Phys. Rev. A: At., Mol., Opt. Phys.*, 2007, **75**, 012502.
33 W.-C. Tung, M. Pavanello and L. Adamowicz, *J. Chem. Phys.*, 2011, **134**, 064117.
34 F. Holka, P. G. Szalay, J. Fremont, M. Rey, K. A. Peterson and V. G. Tyuterev, *J. Chem. Phys.*, 2011, **134**, 094306.

35 R. S. Mulliken, *Phys. Rev.*, 1936, **50**, 1028.
36 M. Nest, F. Remacle and R. D. Levine, *New J. Phys.*, 2008, **10**, 025019.
37 R. Velasco, *Can. J. Phys.*, 1957, **35**, 1204.
38 A. H. Zewail, *Femtochemistry, Ultrafast dynamics of the chemical bond*, World Scientific Publishing Co. Pte. Ltd, Singapore, 1994, vol. I and II.
39 M. Grønager and N. E. Henriksen, *J. Chem. Phys.*, 1996, **104**, 3234.
40 M. Grønager and N. E. Henriksen, *J. Chem. Phys.*, 1998, **109**, 4335.
41 H. Dietz and V. Engel, *J. Phys. Chem. A*, 1998, **102**, 7406.
42 K. B. Møller, N. E. Henriksen and A. H. Zewail, *J. Chem. Phys.*, 2000, **113**, 10477.
43 P. Fuentealba, H. Preuss, H. Stoll and L. Von Szentpály, *Chem. Phys. Lett.*, 1982, **89**, 418.
44 E. Czuchaj, F. Rebentrost, H. Stoll and H. Preuss, *Theor. Chem. Acc.*, 1998, **100**, 117.
45 E. Czuchaj, M. Krośnicki and H. Stoll, *Chem. Phys.*, 2003, **292**, 101.
46 M. Dolg, Effective Core Potentials, in *Modern Methods and Algorithms of Quantum Chemistry*, ed. J. Grotendorst, NIC Series, 2000, vol. 3, p. 507.
47 Unofficial set from D. Feller, see http://www.molpro.net.
48 T. H. Dunning Jr, *J. Chem. Phys.*, 1989, **90**, 1007.
49 H.-J. Werner, P. J. Knowles, G. Knizia, F. R. Manby, M. Schütz, P. Celani, W. Györffy, D. Kats, T. Korona, R. Lindh, A. Mitrushenkov, G. Rauhut, K. R. Shamasundar, T. B. Adler, R. D. Amos, A. Bernhardsson, A. Berning, D. L. Cooper, M. J. O. Deegan, A. J. Dobbyn, F. Eckert, E. Goll, C. Hampel, A. Hesselmann, G. Hetzer, T. Hrenar, G. Jansen, C. Köppl, Y. Liu, A. W. Lloyd, R. A. Mata, A. J. May, S. J. McNicholas, W. Meyer, M. E. Mura, A. Nicklaß, D. P. O'Neill, P. Palmieri, D. Peng, K. Pflüger, R. Pitzer, M. Reiher, T. Shiozaki, H. Stoll, A. J. Stone, R. Tarroni, T. Thorsteinsson and M. Wang, *MOLPRO, version 2012.1, is a package of ab initio programs*, 2012, see http://www.molpro.net.
50 C. E. Moore, *Atomic energy levels as derived from the analysis of optical spectra-Hydrogen through Vanadium*, Circular of the National Bureau of Standards, 467, U. S. Government Printing Office, Washington, 1949, vol. I.
51 L. D. Landau and E. Lifshitz, *Quantum Mechanics*, Pergamon, New York, 1965.
52 K. R. Way and W. C. Stwalley, *J. Chem. Phys.*, 1973, **59**, 5298.
53 D. J. Tannor, *Introduction to quantum mechanics: a time-dependent perspective*, University Science Books, Sausalito, 2007.
54 P. Bilingsley, *Probability and measure*, John Wiley & Sons, New York, Chichester, Brisbane, Toronto, Singapore, 1995.
55 B. Schmidt and U. Lorenz, WavePacket: A Matlab package for numerical quantum dynamics. I: Closed quantum systems and discrete variable representations, *Comput. Phys. Commun.*, 2017, **213**, 223; B. Schmidt and C. Hartmann, *WavePacket: A Matlab package for numerical quantum dynamics. II: Open quantum systems and optimal control*, 2017, manuscript in preparation.
56 M. Dulick, K.-Q. Zhang, B. Guo and P. F. Bernath, *J. Mol. Spectrosc.*, 1998, **188**, 14.
57 Y. L. Huang, W. T. Luh, G. H. Jeung and F. X. Gadea, *J. Chem. Phys.*, 2000, **113**, 683.
58 R. J. Le Roy, LEVEL: a computer program for solving the radial Schrdinger equation for bound and quasibound levels, *J. Quant. Spectrosc. Radiat. Transfer*, 2017, **186**, 167.